Development of Electroplated Magnesium Microstructures for Biodegradable Devices and Energy Sources

Melissa Tsang, *Student Member, IEEE*, Andac Armutlulu, Florian Herrault, *Senior Member, IEEE*, Richard H. Shafer, Sue Ann Bidstrup Allen, and Mark G. Allen, *Fellow, IEEE*

***Abstract*— This paper presents fabrication approaches for magnesium (Mg) microstructures embedded in biodegradable polymers using through-mold Mg electrodeposition and metal-transfer-molding. Biodegradable implantable electronics have garnered increasing interest from the medical community for the monitoring and treatment of transient diseases. Magnesium is a biodegradable metal with desirable properties, and the ability to micropattern Mg thick films (i.e., about >1 μm) with direct microelectromechanical systems (MEMS) integration would support the development of more sophisticated and clinically relevant biodegradable devices and microsystems. Magnesium microstructures were electroplated through micropatterned water-soluble molds in a nonaqueous electrolyte and transfer molded into a biodegradable polymer. Electroplated Mg compared favorably with commercial Mg foil based on elemental composition, crystal orientation, electrical resistivity, and corrosion behavior. Magnesium electroplated to a thickness of up to 50 μm showed a grain size of ∼10 μm, and minimum feature dimensions of 100 μm in width and spacing. Completely biodegradable Mg and poly-L-lactic acid constructs were demonstrated. The application of Mg thick films toward biodegradable energy sources was explored through the fabrication and testing of biodegradable Mg/Fe batteries. The batteries exhibited a capacity and power of up to 2.85 mAh and 39 μW, respectively. Results confirmed the advantages of electrodeposited Mg microstructures for biodegradable MEMS applications. [2014-0103]**

***Index Terms*— Biodegradable, magnesium, fabrication technologies, bioMEMS.**

I. Introduction

THE ELEMENT magnesium (Mg) offers a unique combination of mechanical, electrochemical, electrical, and physiological properties that are attractive for biomedical applications. Magnesium is commonly alloyed with aluminum for structural applications in the automotive and aerospace industries due to its high modulus-to-density ratio [1]–[4]. Magnesium is also the fourth-most common cation found in the human body and an essential mineral nutrient. For example, adenosine triphosphate (ATP), the main energy source in biological cells, requires a bound Mg ion to be biologically active. Magnesium also plays a critical role in stabilizing polyphosphate compounds involved in DNA and RNA synthesis [5], [6]. Further, Mg is an electronegative element with a standard electrode potential of −2.34 V vs. SHE, a theoretical capacity of 2200 mAh/g, and naturally corrodes within a physiological environment [7]–[9]. These unique properties promote the use of Mg for biomedical applications, such as for the development of biodegradable implantable technologies. Biodegradable implants would be advantageous for the treatment and monitoring of transient disease states, such as with bone or wound healing and drug delivery.

To date, biomedical use of Mg has been demonstrated in structural devices, such as biodegradable stents and bone screws, as well as for transient implantable electronics [9]–[14]. The structural devices are typically machined from commercial extruded or cold-rolled Mg, such as with the laser micromachining of Mg foil for biodegradable stents [9], [10]. Fabrication of transient electronics containing Mg relies on the bulk micromachining of commercial Mg and physical vapor deposition (PVD) of thin-film Mg (i.e., <1 μm). However, these current methods of fabricating and patterning Mg for transient electronics have their respective limitations that preclude the full exploitation of Mg for clinically-targeted biodegradable microelectronics. Physical vapor deposition techniques, such as sputtering and evaporation, produce high quality Mg thin films with nanoscale grain size and high purity due to the vacuum deposition conditions. Further, the crystal orientation and morphology, ranging from columnar to granular structure, are tunable based on deposition conditions. Studies have demonstrated the enhanced corrosion resistance of Mg thin films in comparison to bulk commercial cold-rolled Mg [4]–[15]. While these positive qualities render thin-film Mg a good candidate for corrosion resistant coatings, films deposited by PVD methods are typically limited to submicron thicknesses. Due to the kinetics of Mg corrosion in physiological fluids, submicron, unpassivated Mg films biodegrade on the timescale of hours in physiological solutions. Hwang et al. demonstrated that 150-nm-thick Mg resistors completely dissolve in deionized water after 3 hours. Protection of the Mg

Manuscript received March 31, 2014; revised June 25, 2014; accepted September 14, 2014. Date of publication October 13, 2014; date of current version November 25, 2014. Subject Editor D.-I. D. Cho.

M. Tsang is with the School of Biomedical Engineering, Georgia Institute of Technology, Atlanta, GA 30332 USA (e-mail: melissa_tsang@gatech.edu).

A. Armutlulu and S. A. B. Allen are with the School of Chemical and Biomolecular Engineering, Georgia Institute of Technology, Atlanta, GA 30332 USA (e-mail: aarmutlulu3@gatech.edu; sue.bidstrup@chbe.gatech.edu).

F. Herrault and R. H. Shafer are with the School of Electrical and Computer Engineering, Georgia Institute of Technology, Atlanta, GA 30332 USA (e-mail: fh59@gatech.edu; richard.shafer@gatech.edu).

M. G. Allen is with the Department of Electrical and Systems Engineering, University of Pennsylvania, Philadelphia, PA 19104 USA (e-mail: mallen@upenn.edu).

Color versions of one or more of the figures in this paper are available online at http://ieeexplore.ieee.org.

Digital Object Identifier 10.1109/JMEMS.2014.2360201

with barrier oxide (e.g., MgO) and polymeric encapsulation extended longevity of the Mg to approximately 90 hours, though the degradation rate is expected to increase in physiological fluid [13]. Consequently, biodegradable devices comprising thin-film Mg may be restricted to clinical applications that require a monitoring and/ or treatment window of only several days, unless longer-lasting passivation schemes that simultaneously contemplate biodegradation are demonstrated.

The bulk micromachining of commercial Mg overcomes the thickness limitation of PVD methods, but is, in turn, limited in geometry and MEMS-integration. Common methods for the micropatterning of commercial Mg include photochemical etching, laser micromachining, and electric discharge machining (EDM). D.M. Allen et al. demonstrated 300-μm-wide feature and millimeter-scale spacing from the photochemical etching of Mg foil (250 μm thickness) in nitric acid solution, but showed no MEMS integration [16]. We previously demonstrated finer feature width and spacing (i.e., 100 μm) by confining photochemical etching to the top surface of Mg foil mounted onto a carrier substrate and the use of dilute hydrochloric acid. However, the isotropic nature of the chemical etchants limited the minimum feature size for a given thickness of Mg foil, and produced non-vertical sidewalls [17]. In contrast to wet chemical etching techniques, laser micromachining of commercial Mg achieved finer feature size, with 80-μm-wide lines and 20-μm-wide gaps demonstrated from 70-μm-thick Mg foil. However, the redeposition of debris and oxidation on the sidewall of laser-cut structures required post-process chemical treatment. In our previous study, citric acid was used to remove the redeposited material because the etchant preferentially removes metal oxides. However, citric acid will also etch magnesium isotropically via an oxidative mechanism, which, ultimately, reduced the Mg thickness by 15% and increased surface roughness threefold [17]. Boutry et al. utilized EDM to fabricate RLC resonators from 3-mm-thick commercial Mg that featured a width of 1 cm and a gap of 0.6 mm [14]–[18]. As shown, the bulk micromachining of commercial Mg is limited in minimum attainable feature size, amenability to three-dimensional multilayered structures, and post-process integration with other MEMS. While these subtractive microfabrication approaches may be sufficient for certain applications, further advances in Mg microfabrication and integration would support the development of more sophisticated biodegradable devices and systems.

This study presents the development of a MEMS-compatible Mg electrodeposition process for the fabrication of biodegradable bioMEMS, as well as a demonstration of the electrochemical advantages of Mg as a key component of a biodegradable energy source. Specifically, the through-mold electrodeposition of Mg was investigated with an emphasis on (1) ease of integration with traditional MEMS processing and (2) use of biocompatible and non-permanent materials to enable the development of biodegradable MEMS. In contrast to the bulk micromachining of commercial Mg, electrodeposition is an additive approach that enables batch-scale micropatterning of Mg structures with specifically designed patterns. Potentially, the use of multiple electroplating steps enables the development of 3D microstructures, which would be challenging to achieve using the above-mentioned subtractive Mg patterning technologies. Due to its high electronegativity, Mg is difficult to electroplate from an aqueous electrolyte solution. Instead, non-patterned Mg electrodeposition has been demonstrated in organic solutions and ionic liquids, most commonly with Grignard reagents solubilized in ether [7], [19]–[24]. For example, Mg electrodeposition has been used to generate porous deposits of Mg nanoparticles for hydrogen storage applications and non-patterned surface coatings for corrosion-resistance [19]–[25]. However, challenges with Mg electrodeposition have hitherto limited its application to MEMS [17]–[26]. While Mg electrodeposition takes place in a non-aqueous solution, the metal is reactive with protic solvents and water. Hence, pre-plating processing materials (e.g., the electroplating mold) must survive extended immersion in non-aqueous solutions and post-plating processes should avoid prolonged exposure to aqueous solutions. In addition, materials utilized in the fabrication process must either be biocompatible and biodegradable, or easily removable to eliminate the presence of permanent materials in a biodegradable device without exposure to harsh processing conditions that might initiate or significantly accelerate device degradation.

We have previously demonstrated the non-aqueous electrodeposition of aluminum microstructures from lithographically-defined photosensitive polyimide molds [27]. The removal of thick polyimide films required either extensive dry etching in oxygen-based plasmas or wet etching in commercial strippers. Based upon our work on Mg patterning [17] and non-aqueous electrodeposition of Al [27], the present study explores the development of through-mold Mg electroplating with water-soluble molds and on a flexible polyimide substrate to enable the development of completely biodegradable Mg microstructures.

II. Materials and Fabrication

A. MEMS-Based Through-Mold Electrodeposition of Mg

To achieve Mg microstructures, Mg was electrodeposited through a lithographically-defined SU-8 mold. Although SU-8 is not biodegradable, its chemical insolubility in solvents and amenability to lithographic patterning supported the use of SU-8 as the electroplating mold material for preliminary Mg electrodeposition and optimization studies. As shown in Fig. 1a, Ti/Cu/Ti (50 nm/ 500 nm/ 50 nm) was sputter deposited onto a glass substrate and chemically etched through a patterned photoresist mask to obtain a mesh seed layer. Next, photosensitive SU-8 epoxy (SU-8 2025, MicroChem) was used to lithographically define the electroplating mold due to its chemical insolubility in the solvent-based electroplating solution. Briefly, SU-8 was spin-coated to a thickness of 75 μm and soft baked to remove residual solvent. The sample was then physically inverted for backside exposure, where the metallic pattern of the mesh seed layer served as the bright-field mask. Samples were then cross-linked during a post-exposure bake and developed in PGMEA (Thinner Type P). In this manner, the electroplating mold occupied the negative space of the mesh seed layer. Alternatively, for deposition of

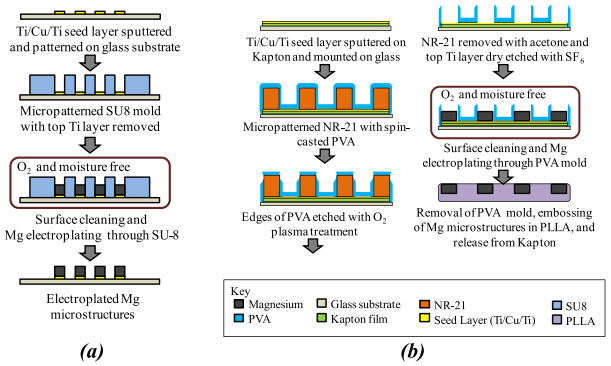

Fig. 1. Fabrication scheme of Mg electroplating through (a) SU-8 and (b) water-soluble PVA molds. Microstructures electroplated through PVA are released from a polyimide (Kapton) substrate and transferred to a biodegradable polymer.

Mg onto a silicon substrate, the SU-8 mold may be aligned to the underlying mesh seed layer through conventional top-side exposure using a lithographic mask. The uppermost Ti of the seed layer was chemically removed in dilute hydrofluoric acid.

The sample was then loaded into an oxygen- and moisture-free glovebox under nitrogen atmosphere and cleaned with salicylic acid solubilized in tetrahydrofuran (THF). The electrodeposition process was conducted in a glovebox because the electrolyte solution is anhydrous and contains strong reducing agents. The measured temperature and relative humidity were approximately 27 °C and <5%, respectively. Commercial Mg foil (250-μm-thick) served as the anode and was mechanically polished with sand paper (2000 grit) and rinsed in THF prior to use. The electrolyte solution comprised 3 M methylmagnesium chloride (CH_3MgCl) in THF. Magnesium was electrodeposited under direct and pulse current at peak current densities of 5, 10, 15, and 20 mA/cm^2 and 20%, 50% and 100% duty cycles to determine optimal plating conditions After electrodeposition, samples were removed, rinsed in THF, and allowed to dry overnight prior to unloading from the glovebox. In subsequent experiments, aluminum chloride ($AlCl_3$) was added to the electrolyte solution, resulting in a 6:1 molar ratio of CH_3MgCl:$AlCl_3$ in THF.

B. Fabrication Process Compatible With Biodegradable MEMS

In this section, polyvinyl alcohol (PVA, MW = 2000 Da) and commercial polyimide film (Kapton, 3-mil-thick) were used as the electroplating mold and substrate, respectively. These materials were selected to enable the use of electrodeposited Mg for biodegradable bioMEMS applications. Specifically, the fabrication process was designed to eliminate the use of non-biodegradable and/or not easily removable materials. For example, the removal of SU-8 by reactive ion etching with O_2 gas can be rather time consuming at thicknesses greater than 10 μm. In contrast, PVA is a water-soluble polymer with poor solubility in non-aqueous solvents, suggesting that it can serve as a mold for non-aqueous electroplating processes and subsequently be removed by solubilizing in water [26]. Moreover, PVA is a FDA-approved, biocompatible polymer that is found in various consumer food products [28]. Kapton film was selected as the substrate to facilitate post-plating substrate removal and packaging with biodegradable material sets [29].

The fabrication process begins with sputter deposition of Ti/Cu/Ti (50 nm/ 500 nm/ 50 nm) onto a 3-mil-thick polyimide film mounted onto a carrier wafer using a thin layer of negative photoresist (Futurrex, NR9-1500PY) (Fig. 1b). This ensured that the bottom surface of the polyimide film was fixed to a rigid carrier during subsequent sonication. The polyimide films were cleaned and briefly treated with oxygen plasma prior to metal deposition. Next, PVA was micropatterned onto the polyimide via a lift-off process using negative-tone photoresist (Futurrex, NR21-20000). The negative image of the desired electroplating mold was lithographically patterned with 100-μm-thick NR-21 and briefly treated with oxygen plasma. PVA solutions were prepared with commercially purchased PVA under constant stirring at 90 °C, which exceeds the glass transition temperature of PVA without exceeding the boiling point of water, until a homogenous solution was achieved. To improve surface wettability, samples were briefly treated with oxygen plasma and a dilute PVA solution (10 wt.%) was spin coated onto the samples. Next, two layers of PVA, at a concentration of 33 wt.%, were spin-coated onto the samples at 1000 rpm for 45 seconds. Samples were dried in an oven at 100 °C for 10 min to remove residual water and cooled to room temperature. To facilitate removal of the NR-21 pattern, samples were treated with reactive ion etching in oxygen gas for five minutes to etch away PVA coating the edges of the NR-21 features. This was performed at 200 mTorr and 200 W with a 5:1 ratio of O_2 and CHF_3 gas. Samples were then sonicated in acetone to remove the negative photoresist, resulting in a micropatterned water-soluble mold. The topmost titanium of the seed layer was dry etched by reactive ion etching in SF_6 gas to prevent exposure of the sample to aqueous etchants. Samples were loaded into the glovebox and electroplated in a 1:6 molar ratio of aluminum chloride and methylmagnesium chloride in a two-electrode-cell configuration. The pulse plating conditions were an average current density of 10 mA/cm^2 and a duty cycle of 20% (t_{on} = 1 ms, t_{off} = 4 ms), which corresponded to a deposition rate of approximately 7 μm/h. After electroplating, samples were rinsed with THF, dried, and removed from the glove box. Magnesium samples were stored within the glovebox unless immediate use was desired to eliminate long-term exposure to ambient conditions.

The PVA mold was removed either by solubilizing in deionized (DI) water or by reactive ion etching with oxygen gas, if dry processing was desired. Magnesium samples were rinsed in isopropranol and thoroughly dried after aqueous removal of the PVA to eliminate residual moisture. In addition, samples were cleaned with 10 wt.% citric acid to remove surface oxidation when necessary. The dry etching of PVA was performed using the reactive ion etching parameters described earlier. Complete removal of the PVA mold was achieved with 25-30 minutes of etching. The Mg microstructures were laminated into prepared 200-μm-thick poly-L-lactic acid (PLLA) sheets with a nanoimprinter (Obducat NIL) in two steps; Mg was embossed into the PLLA at 10 bar and 140 °C for

four minutes and maintained at 10 bar and 70 °C for one minute before cooling down to the demolding temperature (T_{demold} = 30 °C). The polyimide film was peeled from the Mg/PLLA, with the Cu and Ti seed layers selectively adhering to the polyimide. The resulting construct is an example demonstrating the amenability of the PVA and Kapton-based process flow with fabricating biodegradable MEMS.

C. Comparison to Commercially-Purchased Mg Foil

Surface morphology of the electroplated Mg microstructures and PVA molds was characterized by scanning electron microscopy (SEM; Hitachi S-3700 VP-SEM and LEO 1530 FE-SEM). Energy-dispersive x-ray spectroscopy (EDX) was performed to analyze the elemental composition of the Mg deposited from the various electrolyte solutions and plating parameters. Results were compared to elemental composition of commercial pure Mg (CP-Mg). In addition, x-ray diffraction (XRD; Pananalytical XRD) with Cu Kα radiation was used to determine the material composition and crystal orientation of the plated structures. Electrical resistivity of the electroplated Mg was compared to CP-Mg with four-point probe testing (Signatone Four-point Probe). The degradation characteristics of the electroplated and commercial Mg were compared with potentiodynamic testing. Tests were performed with a potentiostat (Wavedriver 10, Pine Instruments) in physiological saline, wherein samples were immersed in the solution for five minutes before testing to come to equilibrium. A three-electrode-cell configuration was implemented with Mg, platinum and silver/silver chloride (Ag/AgCl) as the working, counter and reference electrodes, respectively. Open circuit potentials (OCP) were recorded and linear sweep voltammetry was performed for a 1 V range centered at the measured OCP at a scan rate of 5 mV/s.

D. Application Towards a Biodegradable Mg/Fe Battery

The fabrication and testing of a biodegradable battery, comprising electroplated Mg as the anode and iron (Fe) as the cathode, are presented to demonstrate the application of electroplated Mg to bioMEMS. The electrolyte solution was selected to be 0.1 M magnesium chloride ($MgCl_2$), as the constituent Mg^{2+} and Cl^- ions are found in physiological fluids. The governing chemistry of the biodegradable battery is the galvanic protection of Fe through the anodic oxidation of Mg. The Mg anodes (35-μm-thick) were electroplated through micropatterned PVA molds and released from polyimide substrates as described in the previous section. As the Fe is not consumed during discharge of the battery, Fe cathodes were patterned by e-beam through a shadow mask to a thickness of 300 nm onto glass substrates. Batteries were tested with free-standing Mg anodes and thin-film Fe cathodes immersed into an acrylic electrolyte cell, machined with a CO_2 laser. The use of another material to serve as the current collector for Mg electrodes was avoided because the metal would form a galvanic couple with the Mg upon exposure of the current collector to the electrolyte. Therefore, self-supporting Mg structures were utilized as anodes. Future studies on Mg/Fe biodegradable batteries will address biodegradable packaging and shelf life. Batteries were discharged galvanostatically at discharge currents ranging from 5 to 220 μA with the use of a potentiostat (Model 263, EG&G Princeton Applied Research). The cut-off potential was determined as 200 mV.

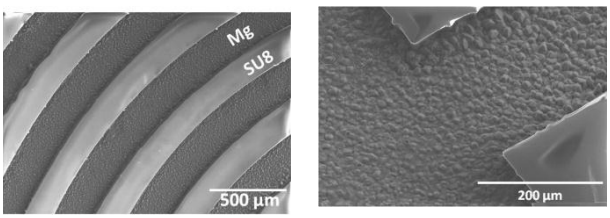

(a) *(b)*

Fig. 2. Electroplated Mg through lithographically defined SU-8 molds: SEM images of surface morphology of (a) an electroplated Mg coil and (b) Mg electroplating adjacent to the SU-8 corner. Samples were plated under pulse current conditions with an average current density of 15 mA/cm^2 at 20% duty cycle to a thickness of 15 μm.

TABLE I
COMPARISON OF THE ELEMENTAL COMPOSITION OF ELECTROPLATED Mg AND COMMERCIAL Mg (CP-Mg), AS DETERMINED BY EDX ANALYSIS

Elemental Composition by EDX			
	Electroplated Mg		CP-Mg
Element	- $AlCl_3$	+$AlCl_3$	
Mg	89%	85%	90%
O	11%	15%	10%
Al	0%	<1%	0%

III. RESULTS AND DISCUSSION

A. Electroplated Mg Microstructures

Magnesium microstructures electrodeposited through lithographically-defined SU-8 molds are shown in Fig. 2. Electroplated Mg coils were plated under pulse current conditions (i_{peak} = 15 mA/cm^2; t_{dep} = 2 h; t_{on} = 0.2 ms, t_{off} = 0.8 ms; 20% duty cycle) in 3 M CH_3MgCl and corresponded to a deposition rate of approximately 7 μm/h. It was observed that the pulse plating condition provided better electrodeposition into the micropatterned SU-8 trenches (i.e., < 300 μm in width), whereas direct current was sufficient for electrodeposition into larger areas. The electroplated Mg microstructures exhibited a thickness of 15 ± 5 μm and a grain size of 10 μm. The measured surface roughness of electroplated Mg was approximately 6 μm, in comparison to the submicron roughness of commercial, cold-rolled Mg foil. The electroplated material demonstrated coherent and dense packing in spite of the surface grain size. EDX analysis determined that the elemental composition at the surface of the electroplated material was 89%Mg and 11%O, which compares favorably to commercial Mg foil (Table I). Electrical resistivity of the electroplated Mg was characterized by conventional four-point DC resistance measurement technique and determined to be 8.7 $\mu\Omega\cdot$cm. For comparison, commercial Mg foil was 5.3 $\mu\Omega\cdot$cm and the reported resistivity of bulk Mg is 4.4 $\mu\Omega\cdot$ cm.

The addition of $AlCl_3$ to the electroplating solution was explored to enhance the quality of the electroplated Mg,

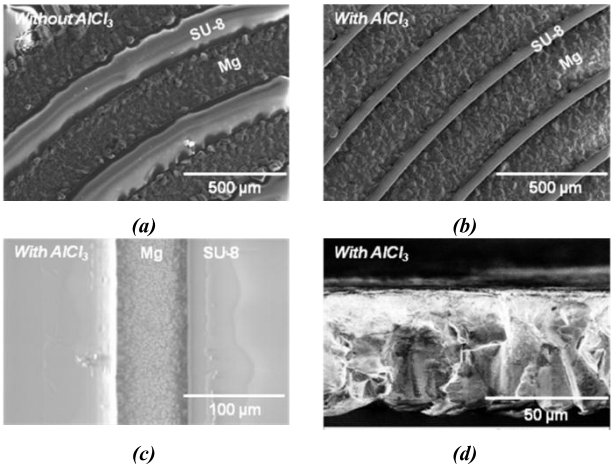

Fig. 3. Comparison of Mg electroplated (a) without and (b-c) with the addition of $AlCl_3$ to the electrolyte solution by VP-SEM, and (d) cross-sectional image of Mg electroplated with the $AlCl_3$ additive. Samples were plated under current-controlled conditions at 15 mA/cm^2 and 20% duty cycle in 250-μm-wide SU-8 trenches to a thickness of (a, b, d) 50 μm and (c) 10 μm.

increase electroplating bath conductivity and hinder electrolyte decomposition (Fig. 3). Studies have suggested that $AlCl_3$ enhances conductivity, voltage stability, and current efficiency of the electroplating bath by increasing ionization of Grignard reagent in ether (e.g., CH_3MgCl in THF). Further, $AlCl_3$ at concentrations below 10:1 molar ratio ($AlCl_3$:CH_3MgCl) has been shown to reduce grain size. Co-deposition of Al was not reported at molar ratios below 3:1 [19]–[28]. Fig. 3 shows the direct comparison of Mg microstructures electroplated in a Grignard reagent solution with and without the addition of $AlCl_3$. The samples were plated to a thickness of 50 μm under identical pulse plating conditions in both electrolyte solutions. For electroplated Mg thicker than 10 μm, the average grain size did not appreciably change along the center of the electroplated region with the addition of $AlCl_3$. However, Mg electroplated in pure CH_3MgCl solution showed preferential plating at the edges of the conductive region, adjacent to the SU-8 mold (Fig. 3a). Surface morphology of Mg plating at the SU-8 border showed larger grains that deformed the SU-8 mold. In contrast, Mg microstructures electroplated in the presence of $AlCl_3$ demonstrated more uniform plating from the center to the edge without any deformation of the adjacent SU-8. Cross-sectional imaging of 50-μm-thick electroplated Mg confirmed the dense crystal packing of Mg microstructures electroplated with $AlCl_3$.

Surface elemental composition of the electroplated material was 85% Mg, 15% O, and insignificant Al, confirming that the addition of $AlCl_3$ did not result in Al co-deposition (Table I). Further, the percentage of Al detected is less than commercial Mg-Al alloys that have been considered for biodegradable, implantable applications. For example, AZ-31 and AZ-91 alloys have been explored for use as biodegradable bone screws and bone plates, and feature 3% and 9% Al, respectively [30]–[32]. The biocompatibility of the AZ-31 has been well demonstrated *in vitro* and *in vivo* [11], suggesting that Al composition equal to or less than that of the alloy may be physiologically tolerated. These findings

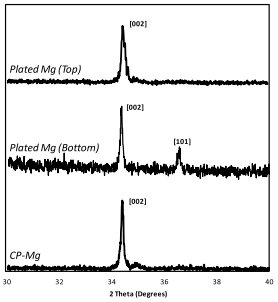

Fig. 4. Comparison of crystal orientation of electroplated Mg and commercial Mg (CP-Mg) based on XRD analysis. Data of plated Mg corresponds to Mg electrodeposited from solution containing $AlCl_3$ as an additive.

suggested that the Al found in the electroplated Mg does not detract from its biocompatibility, though it remains to be validated experimentally. X-ray diffraction was performed on Mg electroplated with the addition of $AlCl_3$ to compare the crystal orientation of the plated material to commercial Mg foil (Fig. 4). The top surface of the 50-μm-thick electroplated Mg showed a singular peak corresponding to the [002] orientation of the hexagonal close packed crystal structure of Mg. The bottom surface showed two strong peaks that corresponded to the [002] and [101] crystal orientation with a (002)/(101) peak intensity ratio of 2.2. This suggested that Mg grown by confined electrodeposition through a mold, under the studied electroplating conditions, shows preferential orientation along the [002] crystal axis. Commercial Mg foil was also analyzed by XRD and exhibited a singular peak between 30° to 40° in the 2θ region that aligned with the [002] peak observed with electroplated Mg samples.

Surface morphology, cross-sectional structure, elemental composition, and crystal orientation results supported that Mg electroplated from a mixture of CH_3MgCl and $AlCl_3$ is comparable to commercial Mg foil. In addition, it was experimentally confirmed that addition of $AlCl_3$ to the plating solution increased the conductivity of the bath and extended its lifetime by hindering electrolyte decomposition. The reduced concentration of CH_3MgCl in the electroplating mixture also rendered the plating solution more transparent, enabling visibility of the sample during the plating process. For these reasons, a 6:1 molar ratio of CH_3MgCl to $AlCl_3$ was exclusively used henceforth as the electrolyte solution for the presented Mg electroplating studies.

B. Fabrication and Integration for Biodegradable MEMS

Unlike traditional photoresists for electroplating, which are susceptible to swelling and dissolution in solvent, we selected a water-soluble material, PVA, for the micropatterning of solvent-resistant molds for Mg electroplating. Using embossing technologies, electroplated Mg microstructures were transfer molded into a biodegradable polymer. Magnesium microstructures electrodeposited through PVA molds, and released and embedded into PLLA are shown in Fig. 5. The presented PVA molds are 75 μm in height and 100 μm in width. Dimensions of the micropatterned PVA are determined by the corresponding NR-21 molds.

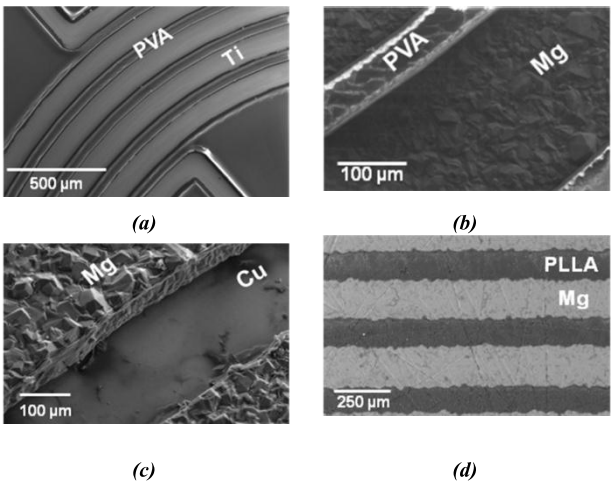

Fig. 5. SEM images of (a) microfabricated water-soluble molds using PVA, (b) electroplated Mg through PVA molds, (c) electroplated Mg after mold removal, and (d) bottom of electroplated Mg after embossing into PLLA and removal from substrate. Image obtained using VP-mode at 30 Pa and backscatter electron detector.

Magnesium structures with thicknesses in the 10 to 100 μm range have been electroplated through micropatterned PVA molds. Thickness of the Mg microstructures was determined by PVA mold height, which was, in turn, limited by thickness of the corresponding NR-21 template. However, this issue may be resolved by replacing NR-21 with thicker negative tone resist (e.g., AZ 125 nXT), which can achieve thicknesses in the hundreds-of-microns range. Magnesium electrodeposited through the PVA molds exhibited uniform thickness across the microstructure, with no dendritic plating observed at the PVA borders (Fig. 5b). The presented Mg microstructures were electroplated through a water-soluble PVA mold and onto a flexible polyimide substrate, in comparison to chemically-resistant SU-8 mold and rigid glass or silicon substrate, to promote the use of Mg electroplating for biodegradable MEMS applications. SU-8, glass, and bulk silicon are not biodegradable materials and their post-plating removal requires either extensive dry etching with oxygen plasma or exposure to corrosive, wet chemicals [34]–[36]. While these processing techniques are common to the microfabrication of traditional MEMS, they are less suitable for the processing of biodegradable MEMS, which are susceptible to corrosion and highly sensitive to chemical and physical conditions. Moreover, prolonged exposure to the solvent electroplating solution (i.e., greater than 4 hours) causes micropatterned SU-8 molds to swell, crack, and delaminate. This often causes adjacent electroplated Mg to either crack or delaminate and places an upper limit on the electrodeposition time per sample. Polyvinyl alcohol overcomes the limitations observed with SU-8, as it is soluble in water and poorly soluble in solvents. It was experimentally verified that micropatterned PVA molds can withstand immersion in the electroplating solution for over 24 hours. Consequently, the PVA molds demonstrated greater chemical resistance to the electroplating solution than SU-8 and ease of removal after Mg electrodeposition by solubilizing in water. This can be shown by the integrity of the PVA mold and removal of the PVA post-plating in Fig. 5b and 5c, respectively. Further, Mg electroplated through PVA molds did not exhibit any cracking.

An alternative approach to water-based PVA removal is by dry etching with oxygen plasma. The spin-casting conditions for the PVA were determined such that the PVA does not entirely fill the trenches created by the micropatterned NR-21. Instead, the PVA coated the bottom substrate and sidewalls of the NR to render a U-shaped horseshoe cross section (Fig. 1b). Hence, a larger surface area of the PVA mold is exposed and the etch depth for complete removal of the PVA is less than that of corresponding SU-8 molds, which feature filled rectangular cross sections. Due to differences in geometry and chemical composition, complete removal of the PVA mold by reactive ion etching can be achieved in 20 minutes with a 5:1 ratio of O_2 and CHF_3 gases, whereas dry etching of corresponding SU-8 molds requires over 1 hour of processing.

The electrodeposition of Mg onto a flexible polyimide substrate facilitated metal-transfer-molding of the Mg microstructures to a biodegradable substrate. After removal of the PVA mold, the Mg microstructures were embossed into PLLA (Fig. 5d). Constant pressure and temperature were applied to the embossed Mg/PLLA construct and after the embossing process, the Mg/PLLA was removed from the non-degradable polyimide by peeling off the flexible substrate. As the Cu and Ti seed layers selectively adhere to the polyimide film due to surface energy principles, no subsequent processing was required to remove these non-degradable metals from the Mg/PLLA construct. EDX analysis indicated that the PLLA embossing process increased oxidation on the electroplated Mg surface by 15%, but did not affect elemental composition of the bulk Mg film. Poly-L-lactic acid (PLLA) was selected as the encapsulation material for proof-of-concept because it is an FDA-approved, commercially-available, and well-studied biodegradable polymer. Microfabrication with PLLA has also garnered interest from the bioMEMS community in recent years [14], [18], [28]. It should be noted that alternative biodegradable polymers may be used for the embossing and encapsulation of Mg. Moreover, the electrodeposition of Mg microstructures through PVA molds and onto polyimide is a modular fabrication process that can be integrated with the prior or subsequent micropatterning of additional biodegradable elements (e.g., Zn, Fe). The PVA molds and flexible substrate provide a versatile approach for the fabrication and integration of electroplated Mg for biodegradable MEMS applications.

C. Degradation Behavior of Electroplated Mg

The degradation characteristics of the electroplated Mg were evaluated electrochemically by potentiodynamic testing. Tests were conducted in phosphate-buffered saline (1x PBS) to emulate the physiological environment and to maintain the solution at the physiological pH (7.4). Fig. 6 shows the polarization curves of electroplated Mg compared against commercial Mg foil. Electroplated Mg demonstrated a corrosion potential of -1.55 V *vs.* SHE, whereas commercial Mg foil showed a corrosion potential of -1.31 V. The difference in corrosion potential suggested that the electroplated Mg

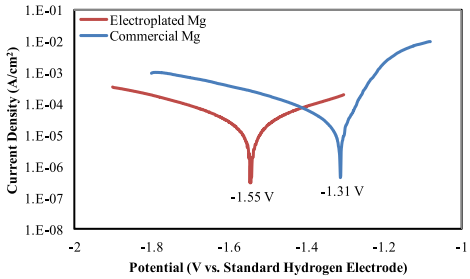

Fig. 6. Corrosion evaluation of electroplated and commercial Mg based on potentiodynamic testing of samples in phosphate-buffered saline (1x PBS).

is less corrosion resistant than commercial foil. This may be attributed to the larger grain size of electroplated Mg, as studies have found that increased surface roughness contributes to increased pitting corrosion in Mg and its alloys. It was speculated that the native passivation layer that forms on the Mg surface, which comprises magnesium hydroxide ($Mg(OH)_2$) in aqueous environments, is more continuous on a smooth surface and provides greater protection against corrosion [3]. Interestingly, electroplated Mg showed a lower corrosion rate than commercial Mg foil. Polarization curves indicated a corrosion current of 24 μA/cm^2 and 67 μA/cm^2 for electroplated Mg and commercial Mg foil, respectively. The fluctuations observed in the anodic curves were attributed to the pitting nature of Mg corrosion, which manifests in the repeated breakdown and formation of the passivation layer. These findings suggested that the corrosion properties of electroplated Mg slightly differ from that of commercial Mg foil. The corrosion resistance of the electroplated Mg may be enhanced by reducing surface roughness, such as by chemical-mechanical polishing or electrochemical polishing, or by surface passivation techniques [2]–[36].

D. Application Towards a Biodegradable Battery

Biodegradable batteries featuring electroplated Mg were fabricated and tested to demonstrate the biomedical applications achievable with Mg. The batteries comprised electroplated Mg and evaporated Fe as the anode and cathode, respectively (Fig. 7). The design of an implantable battery may either consider the physiological solution as the electrolyte or feature an appropriately encapsulated biodegradable electrolyte cell. In the present study, batteries were immersed and discharged in 0.1 M $MgCl_2$ solution to provide preliminary results in support of the latter approach and, more generally, to showcase the use of Mg towards biodegradable energy storage applications. The freestanding Mg anode comprised a circular geometry with a diameter of 5 mm and a thickness of 35 μm. In the present configuration, the Fe cathode was fabricated separately by e-beam evaporation onto a glass substrate. The governing chemistry of the battery, shown in Fig. 7a, is the anodic oxidation of Mg and reduction of hydrogen on the Fe surface. Although the biodegradable nature of Mg and Fe is a key attribute that supports their use in transient medical applications, this feature also results in the parasitic corrosion of Mg and Fe in the chloride-containing electrolyte solution [26], [37]. Consequently, the battery design must also consider the parasitic corrosion of Mg at the anode. The Fe

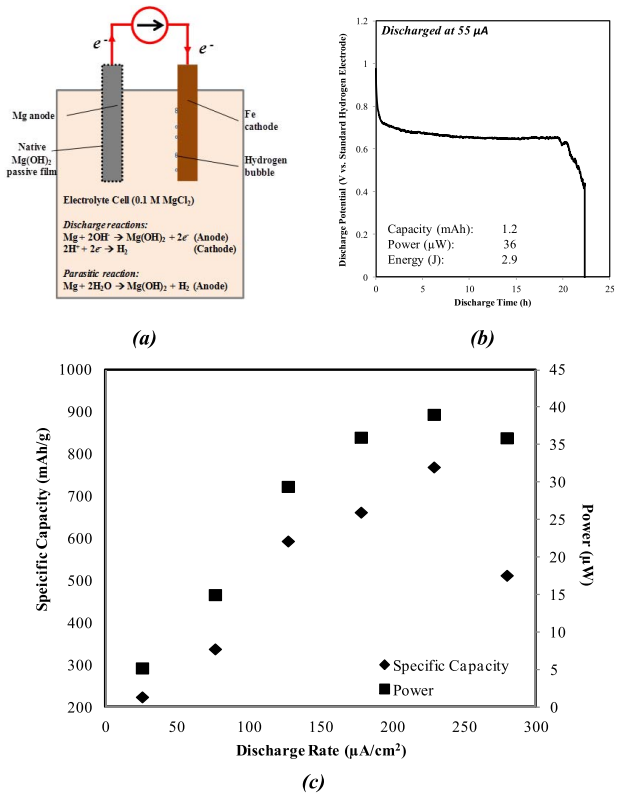

Fig. 7. A MEMS-enabled biodegradable battery comprising electroplated Mg as the anode and evaporated Fe as the cathode in a 0.1 M $MgCl_2$ electrolyte solution. (a) Schematic representation of battery. Electrolyte diffuses across the native magnesium hydroxide ($Mg(OH)_2$) film to reach the Mg surface, where anodic oxidation and parasitic corrosion occur. The formation of $Mg(OH)_2$ from these reactions is countered by mechanical disruption of this passive film from the discharge current. Hydrogen reduction takes place on the Fe cathode surface; (b) Discharge profile of a Mg/Fe battery under galvanostatic discharge at 55 μA; (c) Plot of specific capacity and power *vs.* discharge rate for free-standing Mg/Fe batteries. Tests were performed in a two-electrode cell configuration under galvanostatic discharge.

cathode is galvanically protected by Mg and its corrosion does not occur until the Mg anode is consumed (i.e., after the battery lifetime). Fig. 7b presents the discharge profile of a biodegradable Mg/Fe battery discharged galvanostatically at 55 μA. The biodegradable battery maintained a stable discharge profile with an average discharge potential of 650 mV for 22 hours. At 55 μA discharge, the battery exhibited a capacity, power, and energy of 1.2 mAh, 36 μW, and 2.9 J, respectively.

Interestingly, the specific capacity and power of the electroplated Mg/Fe batteries showed a parabolic trend with respect to discharge rate, as shown in Fig. 7d. While it is not uncommon to observe reduced capacity and power in batteries at higher discharge rates primarily due to transport-related issues of ions, it is speculated that the poor performance observed at low discharge rates is attributed to the corrosion mechanism of Mg. As discussed in the previous section, Mg features a native passivation layer of magnesium hydroxide at the surface. The pitting corrosion of Mg begins when the native hydroxide layer is locally disrupted to expose the underlying Mg. As the corrosion of Mg forms $Mg(OH)_2$ as a reaction product, the surface passivation layer is continually broken down and reformed in pitting zones during the

corrosion process [3], [37]–[39]. When a current is drawn from the Mg/Fe batteries, the native passivation layer is mechanically disrupted to initiate the battery, as well as parasitic corrosion of the anode. At sufficiently low discharge currents, the rate of film breakdown does not overcome the rate of $Mg(OH)_2$ reformation at the anode surface, which prematurely terminates the battery. This was experimentally confirmed by elevating the discharge current from terminated batteries that were discharged at low currents (i.e., 5 μA) to mechanically break through the reformed $Mg(OH)_2$ film and access unused Mg at the anode for a second interval of discharge (data not shown). It was also observed that the shape and peak of the parabolic trend shifted based upon geometry and design of the battery, suggesting that the presented data does not represent the upper limit in Mg/Fe battery performance.

As biodegradable electronics have not yet reached the commercial market, the power requirements of commercial permanent medical implants were considered as a reference in the design of the biodegradable batteries; literature reports power requirement for permanent implants ranging from 10 to 1000 μW depending on the device and application [41]. The present configuration of biodegradable Mg/Fe batteries delivered powers that fell within the range required for commercial medical devices. Design optimization with more application-specific energy requirements will support further developments of biodegradable Mg/Fe batteries.

IV. Conclusion

The present study successfully adapted the non-aqueous electrodeposition of Mg towards the development of biodegradable microstructures for MEMS devices. The fabrication process and materials were developed to overcome the chemical reactivity, susceptibility to corrosion, and aggressive electrodeposition conditions of Mg. Magnesium electroplated from $AlCl_3$-enhanced magnesium-based electrolyte solution showed negligible aluminum (i.e., <1%) and comparable elemental composition to that of commercial Mg foil. Further, through-mold electroplated Mg exhibited similar crystal orientation, electrical resistivity, and corrosion potential to that of commercial Mg, and supported direct MEMS integration and development of completely biodegradable constructs. Biodegradable batteries were fabricated using through-mold electroplated Mg and exhibited viable capacities and powers to support transient implantable devices. The results of this study, from material analyses, fabrication compatibility, and application to bioMEMS, underscore the utility and advantages of through-mold electroplated Mg for the development of biodegradable MEMS.

References

[1] B. Finamore *et al.*, "Development of an implantable biodegradable electrical stimulator for bone repair," in *Proc. Biomed. Eng. Soc. Fall Meeting*, 2009, p. 15213.

[2] J. E. Gray and B. Luan, "Protective coatings on magnesium and its alloys—A critical review," *J. Alloys Compounds*, vol. 336, nos. 1–2, pp. 88–113, Apr. 2002.

[3] R. Walter and M. B. Kannan, "Influence of surface roughness on the corrosion behaviour of magnesium alloy," *Mater. Design*, vol. 32, no. 4, pp. 2350–2354, Apr. 2011.

[4] M. H. Lee, I. Y. Bae, K. J. Kim, K. M. Moon, and T. Oki, "Formation mechanism of new corrosion resistance magnesium thin films by PVD method," *Surf. Coatings Technol.*, vols. 169–170, pp. 670–674, Jun. 2003.

[5] W. J. Fawcett, E. J. Haxby, and D. A. Male, "Magnesium: Physiology and pharmacology," *Brit. J. Anaesthesia*, vol. 83, no. 2, pp. 302–320, Aug. 1999.

[6] N.-E. L. Saris, E. Mervaala, H. Karppanen, J. A. Khawaja, and A. Lewenstam, "Magnesium: An update on physiological, clinical and analytical aspects," *Clin. Chim. Acta*, vol. 294, nos. 1–2, pp. 1–26, Apr. 2000.

[7] D. Aurbach, A. Schechter, M. Moshkovich, and Y. Cohen, "On the mechanisms of reversible magnesium deposition processes," *J. Electrochem. Soc.*, vol. 148, no. 9, p. A1004, 2001.

[8] Y. Yun *et al.*, "Revolutionizing biodegradable metals," *Mater. Today*, vol. 12, no. 10, pp. 22–32, Oct. 2009.

[9] M. Moravej and D. Mantovani, "Biodegradable metals for cardiovascular stent application: Interests and new opportunities," *Int. J. Molecular Sci.*, vol. 12, no. 7, pp. 4250–4270, Jan. 2011.

[10] H. Hermawan, M. Moravej, D. Dubé, M. Fiset, and D. Mantovani, "Degradation behaviour of metallic biomaterials for degradable stents," *Adv. Mater. Res.*, vols. 15–17, pp. 113–118, Feb. 2007.

[11] F. Witte *et al.*, "*In vivo* corrosion of four magnesium alloys and the associated bone response," *Biomaterials*, vol. 26, no. 17, pp. 3557–3563, Jun. 2005.

[12] F. Witte, "The history of biodegradable magnesium implants: A review," *Acta Biomater.*, vol. 6, no. 5, pp. 1680–1692, May 2010.

[13] S.-W. Hwang *et al.*, "A physically transient form of silicon electronics," *Science*, vol. 337, no. 6102, pp. 1640–1644, Sep. 2012.

[14] C. M. Boutry, H. Chandrahalim, and C. Hierold, "Characterization of RF resonators made of biodegradable materials for biosensing applications," *Proc. Eng.*, vol. 25, pp. 1529–1532, Jan. 2011.

[15] K. Schlüter, C. Zamponi, A. Piorra, and E. Quandt, "Comparison of the corrosion behaviour of bulk and thin film magnesium alloys," *Corrosion Sci.*, vol. 52, no. 12, pp. 3973–3977, Dec. 2010.

[16] D. M. Allen, M. Simpkins, and H. Almond, "A novel photochemical machining process for magnesium aerospace and biomedical microengineering applications," *J. Micromech. Microeng.*, vol. 20, no. 10, p. 105010, Oct. 2010.

[17] M. Tsang, F. Herrault, R. H. Shafer, and M. G. Allen, "Methods for the microfabrication of magnesium," in *Proc. 26th IEEE Int. Conf. MEMS*, Taipei, Taiwan, Jan. 2013, pp. 347–350.

[18] C. M. Boutry, H. Chandrahalim, P. Streit, M. Schinhammer, A. C. Hänzi, and C. Hierold, "Towards biodegradable wireless implants.," *Philosoph. Trans. Roy. Soc. A, Math., Phys., Eng. Sci.*, vol. 370, no. 1967, pp. 2418–2432, May 2012.

[19] R. J. Gummow and Y. He, "Morphology and preferred orientation of pulse electrodeposited magnesium," *J. Electrochem. Soc.*, vol. 157, no. 4, pp. E45–E49, 2010.

[20] N. Amir, Y. Vestfrid, O. Chusid, Y. Gofer, and D. Aurbach, "Progress in nonaqueous magnesium electrochemistry," *J. Power Sources*, vol. 174, no. 2, pp. 1234–1240, Dec. 2007.

[21] C. Liebenow, Z. Yang, and P. Lobitz, "The electrodeposition of magnesium using solutions of organomagnesium halides, amidomagnesium halides and magnesium organoborates," *Electrochem. Commun.*, vol. 2, no. 9, pp. 641–645, 2000.

[22] C. Liebenow, "Reversibility of electrochemical magnesium deposition from Grignard solutions," *J. Appl. Electrochem.*, vol. 27, no. 2, pp. 221–225, 1997.

[23] P. Wang, Y. NuLi, J. Yang, and Z. Feng, "Mixed ionic liquids as electrolyte for reversible deposition and dissolution of magnesium," *Surf. Coatings Technol.*, vol. 201, no. 6, pp. 3783–3787, Dec. 2006.

[24] R. D. Rieke and S. E. Bales, "Activated metals. IV. Preparation and reactions of highly reactive magnesium metal," *J. Amer. Chem. Soc.*, vol. 96, no. 26, pp. 1775–1781, 1972.

[25] S. Ben Hassen, L. Bousselmi, E. M. Rezrazi, P. Berçot, and E. Triki, "Comparative study of protective magnesium deposit behaviour obtained by continuous and pulsed currents from methylmagnesium chloride solution," *Surf. Coatings Technol.*, vol. 202, no. 15, pp. 3579–3584, Apr. 2008.

[26] M. Tsang, A. Armutlulu, A. Martinez, F. Herrault, S. A. B. Allen, and M. G. Allen, "A MEMS-enabled biodegradable battery for powering transient implantable devices," in *Proc. IEEE 27th Int. Conf. MEMS*, San Francisco, CA, USA, Jan. 2014, pp. 358–361.

[27] A. B. Frazier and M. G. Allen, "Uses of electroplated aluminum for the development of microstructures and micromachining processes," *J. Microelectromech. Syst.*, vol. 6, no. 2, pp. 91–98, Jun. 1997.

[28] S. K. Saxena, "Polyvinyl alcohol (PVA)," in *Proc. 61st JECFA, Chem. Tech. Assess.*, vol. 1. 2004, pp. 1–3.
[29] M. Luo, A. W. Martinez, C. Song, F. Herrault, and M. G. Allen, "A microfabricated wireless RF pressure sensor made completely of biodegradable materials," *J. Microelectromech. Syst.*, vol. 23, no. 1, pp. 4–13, Feb. 2014.
[30] T. D. Gregory, R. J. Hoffman, and R. C. Winterton, "Nonaqueous electrochemistry of magnesium," *J. Electrochem. Soc.*, vol. 137, no. 3, pp. 775–780, 1990.
[31] F. Witte *et al.*, "Degradable biomaterials based on magnesium corrosion," *Current Opinion Solid-State Mater. Sci.*, vol. 12, nos. 5–6, pp. 63–72, 2008.
[32] P. Gunde, "Biodegradable magnesium alloys for osteosynthesis—Alloy development and surface modifications," Ph.D. dissertation, Dept. Mater., ETH Zürich, Zürich, Switzerland, ETH dissertation no. 19171, 2010.
[33] Y. Xin, C. Liu, X. Zhang, G. Tang, X. Tian, and P. K. Chu, "Corrosion behavior of biomedical AZ91 magnesium alloy in simulated body fluids," *J. Mater. Res.*, vol. 22, no. 7, pp. 2004–2011, 2007.
[34] P. M. Dentinger, W. M. Clift, and S. H. Goods, "Removal of SU-8 photoresist for thick film applications," *Microelectron. Eng.*, vols. 61–62, pp. 993–1000, Jul. 2002.
[35] A. Kono, Y. Arai, Y. Goto, and H. Horibe, "Removal of SU-8 resists using hydrogen radicals generated by tungsten hot-wire catalyzer," *Proc. SPIE, Adv. Etch Technol. Nanopatterning*, vol. 8328, pp. 83280R-1–83280R-10, Mar. 2012.
[36] J. Tang, S. R. Green, and Y. B. Gianchandani, "Miniature wireless resonant rotary motor actuated by lithographically micromachined magnetoelastic foil," in *Proc. Conf. Solid-State Sens., Actuators, Microsyst. Workshop*, 2012, pp. 86–89.
[37] C. Blawert, W. Dietzel, E. Ghali, and G. Song, "Anodizing treatments for magnesium alloys and their effect on corrosion resistance in various environments," *Adv. Eng. Mater.*, vol. 8, no. 6, pp. 511–533, Jun. 2006.
[38] T. Reddy, *Linden's Handbook of Batteries*, 4th ed. New York, NY, USA: McGraw-Hill, 2011, pp. 146–173.
[39] J. E. Oxley, R. J. Ekern, K. L. Dittberner, P. J. Spellman, and D. M. Larsen, "Magnesium dry cells," in *Proc. IEEE 35th Int. Power Sour. Symp.*, Jun. 1992, pp. 18–21.
[40] B. V. Ratnakumar, "Passive films on magnesium anodes in primary batteries," *J. Appl. Electrochem.*, vol. 18, no. 2, pp. 268–279, Mar. 1988.
[41] X. Wei and J. Liu, "Power sources and electrical recharging strategies for implantable medical devices," *Frontiers Energy Power Eng. Chin.*, vol. 2, no. 1, pp. 1–13, Mar. 2008.

Melissa Tsang received the B.S. degree in biomedical engineering from Brown University, Providence, RI, USA, in 2011, with a focus on the design of biomaterials for bladder cancer applications. As a Research Intern with the Division of Preclinical Orthopaedic at Genzyme, Cambridge, MA, USA, her research focused on evaluating the pharmacodynamics of commercially-available treatments for focal chondral defects. She is currently pursuing the M.S. degree in electrical and computer engineering, and the Ph.D. degree in biomedical engineering with the Georgia Institute of Technology, Atlanta, GA, USA. Drawing upon her interests in biomaterials and orthopaedics, she is developing microfabrication technologies for biodegradable materials and implementing these approaches toward designing biodegradable implantable devices for bone healing applications.

Andac Armutlulu received the B.S. and M.S. degrees in chemical engineering from Bogazici University, Istanbul, Turkey, in 2007 and 2009, respectively, and the Ph.D. degree in chemical engineering from the Georgia Institute of Technology, Atlanta, GA, USA, in 2014, with a focus on the design and fabrication of deterministically engineered high-power density energy storage devices enabled by MEMS technologies and electrochemical techniques. His other research interests include applied electrochemistry, micro and nano fabrication technologies, biodegradable power sources, and carbon dioxide capture. He is currently a Post-Doctoral Fellow with ETH Zurich, Zurich, Switzerland.

Florian Herrault (SM'14) received the B.S. and M.S. degrees in physics and materials science from the National Institute of Applied Sciences, Toulouse, France, in 2003 and 2005, respectively, and the Ph.D. degree in electrical and electronics engineering from the University of Toulouse, Toulouse, in 2009. From 2009 to 2013, he was a Research Engineer with the MicroSensors and MicroActuators Group, Georgia Institute of Technology, Atlanta, GA, USA, where he acted as the Deputy Director. His research was focused on integrated magnetics for power supplies on a chip and MEMS-based biomedical implants. He is currently a member of the technical staff with HRL Laboratories, Malibu, CA, USA, where he is developing advanced microfabrication-based packaging technologies for millimeter-wave components. He has been a Technical Program Committee Member and the Session Co-Chair of the International Workshop on Power Supply on Chip in 2010 and 2012; the International Workshop on Micro and Nanotechnology for Power Generation and Energy Conversion Applications in 2012 and 2013; and the Solid-State Sensors, Actuators, and Microsystems Workshop in 2014.

Richard H. Shafer received the degree in electrical engineering from the University of Kentucky, Lexington, KY, USA. He has over 20 years of significant technical experience in diverse research and manufacturing environments. He has a broad technical background with particular expertise in analysis, characterization, processing, and fabrication of ceramic materials; refractory metals; vacuum technology; and electrical, electronic, and mechanical design and automation. He was with the vacuum tube industry for over 15 years, and has knowledge of process procedures, lab procedures, microscopy—both electron and optical—vacuum systems. He has an extensive knowledge in the design, production, and testing of thermionic emitters. As the Laboratory Manager of the Microelectromechanical Systems Group with the Georgia Institute of Technology, Atlanta, GA, USA, he maintains the labs and provides support for the people using them.

Sue Ann Bidstrup Allen received the B.S. degree from the Massachusetts Institute of Technology, Cambridge, MA, USA, and the Ph.D. degree in chemical engineering from the University of Minnesota, Minneapolis, MN, USA. She was a Professor with the School of Chemical and Biomolecular Engineering, Georgia Institute of Technology, Atlanta, GA, USA, for 26 years. In 2014, she joined the faculty of the Department of Chemical and Biomolecular Engineering at the University of Pennsylvania, Philadelphia, PA, USA. Her research interests intersect the areas of polymer engineering, microelectronic materials, and processing. She was a recipient of the National Science Foundation Presidential Young Investigator Award, the DuPont Young Faculty Award, the American Society for Engineering Education Sharon Keillor Award, and the Council of Chemical Research Diversity Award. She is a Fellow of the Society of Plastic Engineers.

Mark G. Allen (M'88–SM'04–F'11) received the B.A. degree in chemistry, the B.S.E. degree in chemical engineering, and the B.S.E. degree in electrical engineering from the University of Pennsylvania, Philadelphia, PA, USA, and the M.S. and Ph.D. degrees from the Massachusetts Institute of Technology, Cambridge, MA, USA, in 1989. In 1989, he joined the faculty of the School of Electrical and Computer Engineering, Georgia Institute of Technology (Georgia Tech), Atlanta, GA, USA, where he holds the rank of Regents' Professor and the J.M. Pettit Professorship in Microelectronics, and a joint appointment with the School of Chemical and Biomolecular Engineering. In 2013, he became the Alfred Fitler Moore Professor of Electrical and Systems Engineering and the Scientific Director of the Singh Nanotechnology Center at the University of Pennsylvania. His research interests are in the development and the application of new micro and nano fabrication technologies, and MEMS. He was the Editor-in-Chief of the *Journal of Micromechanics and Microengineering*, and the Co-Chair of the IEEE/ASME MEMS Conference.